Available online at www.sciencedirect.com
SCIENCE DIRECT®
International Journal of Heat and Mass Transfer 49 (2006) 3879–3883
International Journal of HEAT and MASS TRANSFER
www.elsevier.com/locate/ijhmt

Experimental study on thermal characteristics of suspended platinum nanofilm sensors

Xing Zhang [a,*], Huaqing Xie [a], Motoo Fujii [a], Koji Takahashi [b], Tatsuya Ikuta [b], Hiroki Ago [a], Hidekazu Abe [c], Tetsuo Shimizu [c]

[a] *Institute for Materials Chemistry and Engineering, Kyushu University, Kasuga 816-8580, Japan*
[b] *Graduate School of Engineering, Kyushu University, Fukuoka 812-8581, Japan*
[c] *Nanotechnology Research Institute, National Institute of Advanced Industrial Science and Technology, Tsukuba 305-8562, Japan*

Received 4 April 2005
Available online 21 June 2006

Abstract

In this paper, the thermal characteristics of suspended platinum (Pt) nanofilm sensors have been investigated experimentally. The Pt nanofilm sensors with the thickness of 28–40 nm, the width of 260–601 nm, and the length of 5.3–5.7 μm were fabricated by electron beam lithography, electron beam physical vapor deposition and isotropic/anisotropic etching processes. Based on the one-dimensional heat conduction model, the in-plane thermal conductivity of the nanofilm sensors was obtained from the linear relation of the volume-averaged temperature increase and the heating rate measured in vacuum. Furthermore, natural convection heat transfer coefficients of air around the suspended nanofilm sensors at the pressures ranging from 1×10^{-2} Pa to 1 atm were also investigated. The experimental results show that the in-plane thermal conductivities of the nanofilm sensors are much lower than those of the bulk values, the natural convection heat transfer coefficients are, however, very high at the atmospheric pressure.

Keywords: Heat transfer coefficient; Nanosensor; Suspended nanofilm; Thermal conductivity

1. Introduction

One-dimensional (1D) nanostructures such as carbon nanotubes [1] and semiconductor nanowires [2] have received considerable attention due to their potential applications in electronic, optical and energy conversion devices. The electrical and mechanical properties have been investigated at a single nanotube level. The thermal properties of carbon nanotubes are also of interest for basic science as well as for technological applications. However, most of the studies only include estimating the thermal properties of carbon nanotubes from the experiments of micrometer-/millimeter-sized mats of carbon nanotubes. Kim et al. [3] first developed a microdevice containing two suspended independent heater islands to probe the thermal transport of multiwall carbon nanotube (MWCNT). However, it is hard to estimate the error in their measurements. Zhang et al. [4] proposed a method using a sample-attached T-type sensor that is able to measure the thermal conductivity of a single carbon fiber, metallic and non-metallic wire. The method has been developed and successfully used to measure the thermal conductivity of one single carbon fiber with a diameter of 10 μm or less [5]. Based on the method, we recently proposed to use a sample-attached T-type suspended nanosensor to measure the thermal conductivity of one single multiwall carbon nanotube or a bundle of a few single-wall carbon nanotubes. In the measurements, the sample of a fiber, tube or wire as a pin fin is attached to a short hot wire that is supplied with a constant direct current to generate a uniform heat flux. Based on the analysis of one-dimensional steady-state heat conduction along the wire and the attached sample, the thermal conductivity of sample can be determined when

* Corresponding author. Tel./fax: +81 92 583 7638.
E-mail address: xzhang@cm.kyushu-u.ac.jp (X. Zhang).

0017-9310/$ - see front matter © 2006 Elsevier Ltd. All rights reserved.
doi:10.1016/j.ijheatmasstransfer.2006.04.016

the average temperature rise and the heat generation rate of the hot wire are measured. The method is considered to have the advantages of simplicity as well as high accuracy. However, because of the small size of carbon nanotubes, the hot wire should be fabricated at nanoscale to obtain sufficient sensitivity. As known, the thermal properties of nanoscale materials are very different from bulk values due to the structure defect and boundary scattering [6–9]. Large errors would take place if the bulk values were taken for the thermal properties for the nanosized hot-wire in the measurements and calculations. Therefore it is essential to determine the thermal characteristics for the nanofilm sensors in our experiments for measuring the thermal conductivity of one single carbon nanotube.

The objectives of the present work are to investigate the thermal characteristics of the nanofilm sensors fabricated by electron beam (EB) lithography, electron beam physical vapor deposition (EBPVD) and isotropic/anisotropic etching techniques. The thermal conductivities of the nanofilm sensors are determined by a one-dimensional heat conduction method. Furthermore, natural convection heat transfer coefficients at a wide pressure range are also investigated in order to determine the effect of pressure on measurement accuracy of the thermal conductivity of a single carbon nanotube by the nanofilm sensors.

2. Experiments

Fig. 1 shows a schematic diagram of the nanofilm sensor and the scanning electron microscope (SEM) image of the nanofilm marked by a circle in the left figure. Seven nanofilm sensors with the thickness of 28–40 nm, the width of 260–601 nm, and the length of 5.3–5.7 μm were made in the present study. The fabrication processes include EB lithography, EBPVD and isotropic/anisotropic etching techniques as shown in Fig. 2. A Si(100) substrate with a SiO_2 layer of 180 nm thickness is used as the starting material. First, an electron beam resist layer is spin-coated to be 320 nm thick. By using an electron beam lithography system, the patterns of nanofilm and the leads are directly drawn on the EB resist. In the next step, a titanium film of 5 nm and a platinum film of 28–40 nm are deposited subsequently by the EBPVD method. The titanium film is only for adhesion. Then a lift-off technique is applied,

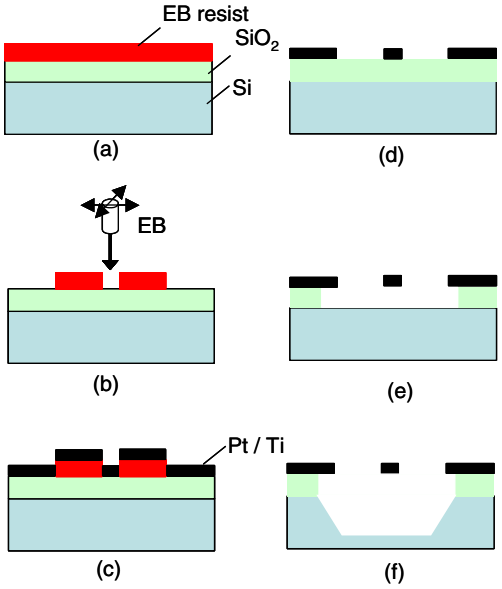

Fig. 2. Fabrication processes of nanofilm sensor.

where the chip is immersed in a liquid resist-remover to leave only the Pt/Ti pattern on the SiO_2 layer. An isotropic etching using a buffered hydrofluoric acid is applied to remove the SiO_2 layer around the Pt nanofilm. The titanium layer is also etched away in this process. The Si is partly etched using KOH solution in order to detach the nanofilm from the substrate. In the present study, the gap between the nanofilm and substrate is about 6 μm, and the Pt film is not etched by the buffered hydrofluoric acid and KOH solution.

Fig. 3 shows an electrical circuit for measuring the electrical and thermal properties. In the measurements of the temperature coefficient of resistance, the silicon wafers with the nanofilm sensors were placed in a constant temperature bath and the electrical resistances R, at different temperatures, were measured using a four-wire technique (see Fig. 3). The temperature coefficient of resistance (β) is determined by the following formula:

$$\beta = \frac{R - R_0}{R_0(T - T_0)} \tag{1}$$

where R_0 is the resistance at temperature T_0.

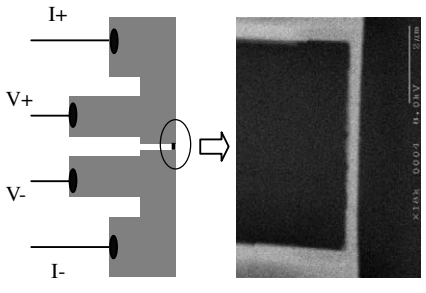

Fig. 1. Schematic diagram of the nanofilm sensor and SEM image of the suspended nanofilm.

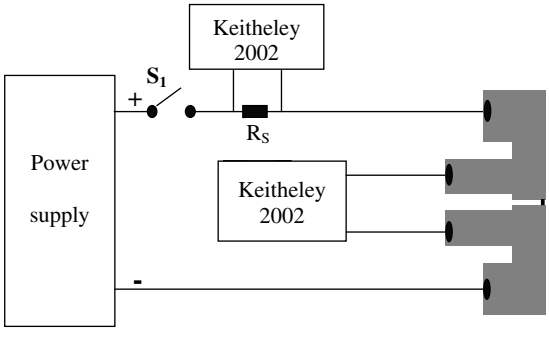

Fig. 3. Schematic drawing of the electrical circuit.

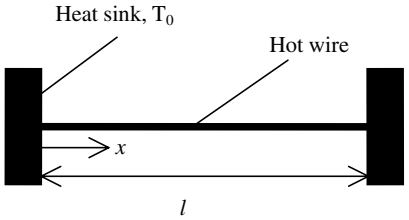

Fig. 4. Physical model of heat transfer in nanofilm sensor.

In the measurements of the thermal properties, the nanofilm sensor serves both as a heating source with homogeneous heat generation rate and as a resistance thermometer. Initially the nanofilm sensor and its connectors keep at thermal equilibrium at T_0. When a constant heating current flows through the nanofilm sensor, the nanofilm sensor is heated and subjected to one-dimensional heat transfer. The physical model is shown in Fig. 4. The non-dimensional heat transfer equation is expressed as

$$\frac{\partial\theta}{\partial Fo} = \frac{\partial^2\theta}{\partial X^2} - 2\eta Bi\theta + 1 \tag{2}$$

where $\theta = (T - T_0)/(q_v r_h^2/\lambda)$ is the dimensionless temperature rise, $Fo = \alpha t/r_h^2$ Fourier number, $r_h = \sqrt{(wd)/\pi}$ the specified radius, $Bi = hr_h/\lambda$ Biot number, $\eta = (w + d)/\pi r_h$ the shape factor, and $X = x/r_h$ the dimensionless length. In these dimensionless parameters, λ and α are the thermal conductivity and thermal diffusivity, respectively. l, w, and d are the length, width, and thickness, respectively. q_v is the Joule heat per unit volume and h is the heat transfer coefficient which includes the effects of the natural convection and radiation. The initial conditions are given as

$$Fo = 0, \quad \theta = 0 \tag{3}$$

and the boundary conditions are given as

$$X = 0, \quad \theta = 0 \tag{4a}$$

and

$$X = L/2, \quad \frac{\partial\theta}{\partial X} = 0 \tag{4b}$$

Eq. (2) was solved numerically using a finite difference method under the above initial and boundary conditions. Calculated results show that the temperature distribution in a nanofilm sensor with a specified radius 80 nm reaches steady-state after heating for 4 μs, which indicates it is reasonable to adopt steady-state heat transfer in the nanofilm sensor in our measurements. The radiation heat loss is negligible because the experiment temperature is only about 300 K. When the nanofilm sensor is heated in vacuum, there is no natural convection and the nanofilm sensor appears as one-dimensional steady-state heat conduction. The analytical solution for Eq. (2) without the transient term and convection term is obtained and the dimensionalized volume-averaged temperature rise (ΔT_V) is expressed by the heating rate (q), the sensor dimensions, and the thermal conductivity (λ) as

$$\Delta T_V = \frac{q}{\lambda} \times \frac{l}{12wd} \tag{5}$$

Therefore, the thermal conductivity is given as

$$\lambda = \frac{q}{\Delta T_V} \times \frac{l}{12wd} \tag{6}$$

Once the thermal conductivity of a nanofilm sensor is determined from the relation between ΔT_V and q measured in vacuum, based on the analytical solution of Eq. (2) without the transient term, the natural convection heat transfer coefficient can further be obtained from the relation between ΔT_V and q measured at a given pressure.

3. Results and discussion

Table 1 shows the dimensions of seven nanofilm sensors in the present study. The width and length of the nanosensor are measured with a scanning electron microscope and the film thickness is measured with a calibrated quartz crystal thin-film thickness monitor (CRTM-7000 with the resolution of 0.01 nm). The error caused by the dimension measurements is estimated to be less than ±3%.

The linear relation between the electrical resistance and temperature for a representative nanofilm sensor is shown in Fig. 5. The electrical resistance at the corresponding temperature is measured by supplying a small current of about 7 μA to the nanofilm sensor where the self-heating rate caused by the small current is about 8.9×10^{-9} W, and the temperature rise of the nanofilm even in vacuum is also below 0.0085 K. Using least-squares fit, the slope of R to T was determined and β was calculated by Eq. (1).

Table 1
Dimensions of seven nanofilm sensors

Sample	l (μm)	w (nm)	d (nm)
A	5.67	362	40.0
B	5.58	381	40.0
C	5.56	424	40.0
D	5.50	439	40.0
E	5.61	601	40.0
F	5.37	332	27.5
G	5.30	260	27.5

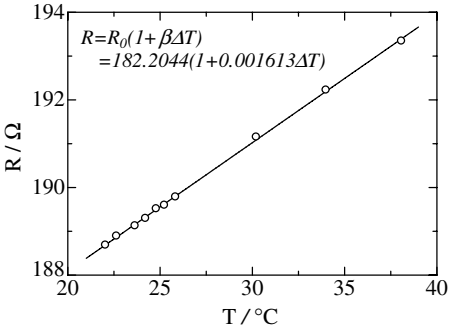

Fig. 5. Dependence of the resistance on the temperature for the nanofilm sensor D.

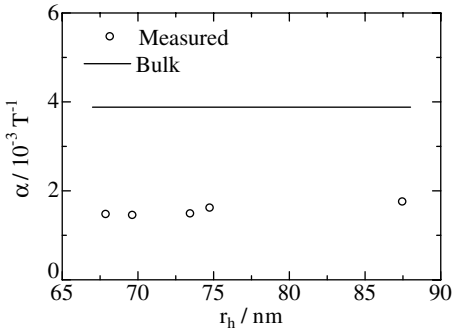

Fig. 6. Resistance–temperature coefficient of the nanofilm sensors A–E.

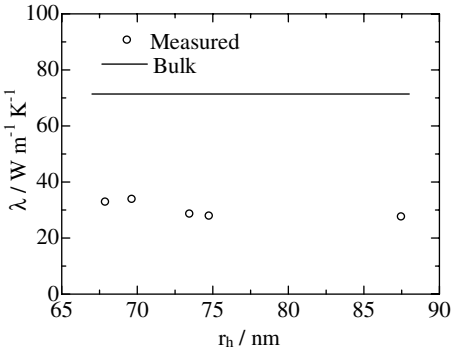

Fig. 8. Thermal conductivity of the nanofilm sensors A–E.

Fig. 6 shows the resistance–temperature coefficients of the nanofilm sensors A–E and the bulk value. The temperature coefficient of resistance of the nanosensors A–E, which is about 0.0015 K^{-1}, is less than half of that of the bulk value of 0.0039 K^{-1}.

When subjected to different current, the nanofilm sensor is heated to different temperature that can be determined from the measurement of the electrical resistance using the following expression

$$\Delta T = \frac{R - R_0}{R_0 \beta} \tag{7}$$

The volume-averaged temperature rise of the nanofilm sensor as a function of heating rate is shown in Fig. 7. It is clearly seen that the temperature rise at atmospheric pressure is much lower than that in vacuum at the same heating rate, indicating that the effect of natural convection is significant. The slope of ΔT_V to q is determined by linear fit of the experimental data and the thermal conductivity of nanofilm sensor is determined from Eq. (6). The thermal conductivities of the nanosensors A–E together with that of bulk value are presented in Fig. 8. It is obvious that the measured thermal conductivities of all the five nanofilm sensors are much lower than that of bulk value. The bulk value of the thermal conductivity of Pt is 71.4 W m^{-1} K^{-1}, whereas those of the experiments are 27.7–33.6 W m^{-1} K^{-1}, less than half of the bulk value. The measurement uncertainty of the thermal conductivity may come from the measurement errors of the voltage, the current, the temperature, and the dimensions of the nanosensor, and it is estimated to be within ±5%. The low values of the thermal conductivity for the thin-films could be attributed to the structure defect, surface scattering, grain boundary scattering, film sizes, fabrication methods, etc. Because it is very difficult to determine which is the main cause of the low values, the measured thermal conductivities are regarded as the special values for the present nanofilm sensors.

The natural convection heat transfer coefficients for the nanofilm sensors A–E at atmospheric pressure are shown in Fig. 9. The solid line shows the results of natural convection heat transfer around a long horizontal thin wire in air [10]. The dashed line shows the limit of pure heat conduction for a small sphere where the Rayleigh number based on the spherical diameter is negligibly small [11]. The dotted line in Fig. 9 is obtained by the least-squares fit of the measured results. The present results are higher than those obtained from a long horizontal thin wire due to the effect of aspect ratio ($l/(2r_h) = 32$–42), but lower than those obtained from the limit of pure heat conduction for the sphere with the corresponding radius. The present heat transfer coefficient decreases slightly with an increase in the specified radius. This tendency is the same as that of a long horizontal thin wire.

Fig. 10 shows the natural convection heat transfer coefficients for the nanofilm sensors F and G at the pressures ranged from 1×10^{-2} Pa to 1 atm. The convective heat

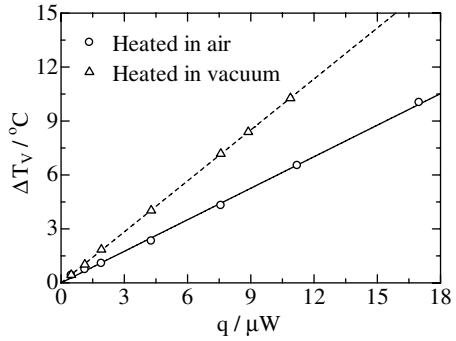

Fig. 7. Temperature rise as a function of heating rate (nanosensor A).

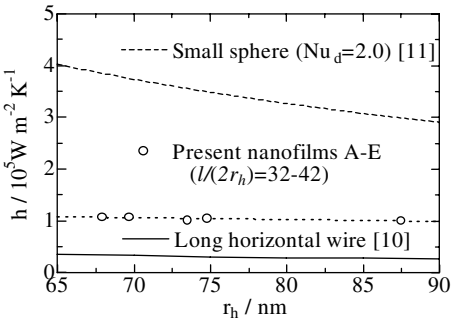

Fig. 9. Heat transfer coefficient of the nanofilm sensors A–E.

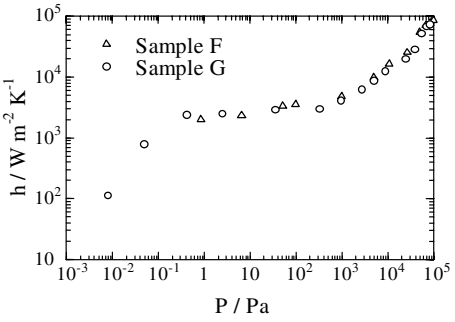

Fig. 10. Effect of pressure on heat transfer coefficient of the suspended nanofilm sensors F and G.

transfer coefficients of two nanofilm sensors agree well each other, and decrease at different slopes in three pressure ranges, that is, the pressure over 10^3 Pa, between 1 and 10^3 Pa, and below 1 Pa. These results are important to determine the effect of pressure on measurement accuracy of the thermal conductivity of a single carbon nanotube by the sample-attached T-type suspended nanosensor.

4. Conclusions

The thermal characteristics of the suspended platinum nanofilm nanosensors have been investigated experimentally. The in-plane thermal conductivities of these films were shown to be less than half of the bulk value. The temperature coefficients of resistance of these nanosensors are much smaller compared to the bulk data. On the other hand, the natural convection heat transfer coefficient is intriguingly high at atmospheric pressure and it decreases rapidly with the decrease of pressure. The present measurements enable us to proceed to measure the thermal conductivity of a single carbon nanotube.

Acknowledgments

This work is supported partly by the Grant-in-Aid for Scientific Research B15360114 from the Ministry of Education, Science, Sports and Culture of Japan.

References

[1] S. Iijima, Helical microtubules of graphitic carbon, Nature 354 (1991) 56–58.
[2] L.D. Hicks, M.S. Dresselhaus, Thermoelectric figure of merit of a one-dimensional conductor, Phys. Rev. B 47 (1993) 16631–16634.
[3] P. Kim, L. Shi, A. Majumdar, P.L. McEuen, Thermal transport measurements of individual multiwalled nanotubes, Phys. Rev. Lett. 87 (2001). Art. No. 215502.
[4] X. Zhang, S. Fujiwara, M. Fujii, Short-hot-wire method for the measurement of the thermal conductivity of a fine fibre, High Temp.–High Press. 32 (2000) 493–500.
[5] X. Zhang, S. Fujiwara, M. Fujii, Measurements of thermal conductivity and electrical conductivity of a single carbon fiber, Int. J. Thermophys. 21 (2000) 965–980.
[6] S.R. Mirmira, L.S. Fletcher, Review of the thermal conductivity of thin films, J. Thermophys. Heat Transfer 12 (1998) 121–131.
[7] D.G. Cahill, W.K. Ford, K.E. Goodson, G.D. Mahan, A. Majumdar, H.J. Maris, R. Merlin, S. Phillpot, Nanoscale thermal transport, J. Appl. Phys. 93 (2003) 793–818.
[8] T. Yamane, S. Katayama, M. Todoki, Importance of basic technology, reference materials, and reference data for thermophysical property measurements on the development of the advanced materials, in: Proceedings of the 24th Japan Symposium on Thermophysical Properties, 2003, pp. 26–28.
[9] S. Kumar, G.C. Vradis, Thermal-conductivity of thin metallic-films, J. Heat Transfer 116 (1994) 28–34.
[10] T. Fujii, M. Fujii, T. Honda, Theoretical and experimental studies of the free convection around a long horizontal thin wire in air, in: Proceedings of the 7th International Heat Transfer Conference, vol. 2, 1982, pp. 311–316.
[11] M. Fujii, H. Takamatsu, T. Fujii, A numerical analysis of free convection around an isothermal sphere (effects of sphere and Prandtl number), in: Proceedings of the ASME–JSME Thermal Engineering Joint Conference, 1987, pp. 55–60.